Phononic Energy Transport at Differential Material Nanoscales

Antoine Khater

CEA, U Paris 6, Le Mans U

email: **antoine.khater@univ-lemans.fr**

GDR Workshop, Rennes November 2023

Scales for phonons in ultrathin films, multilayers, nanojunctions,..

phonon vibration amplitudes are ~ 0.04 Å at room temperature

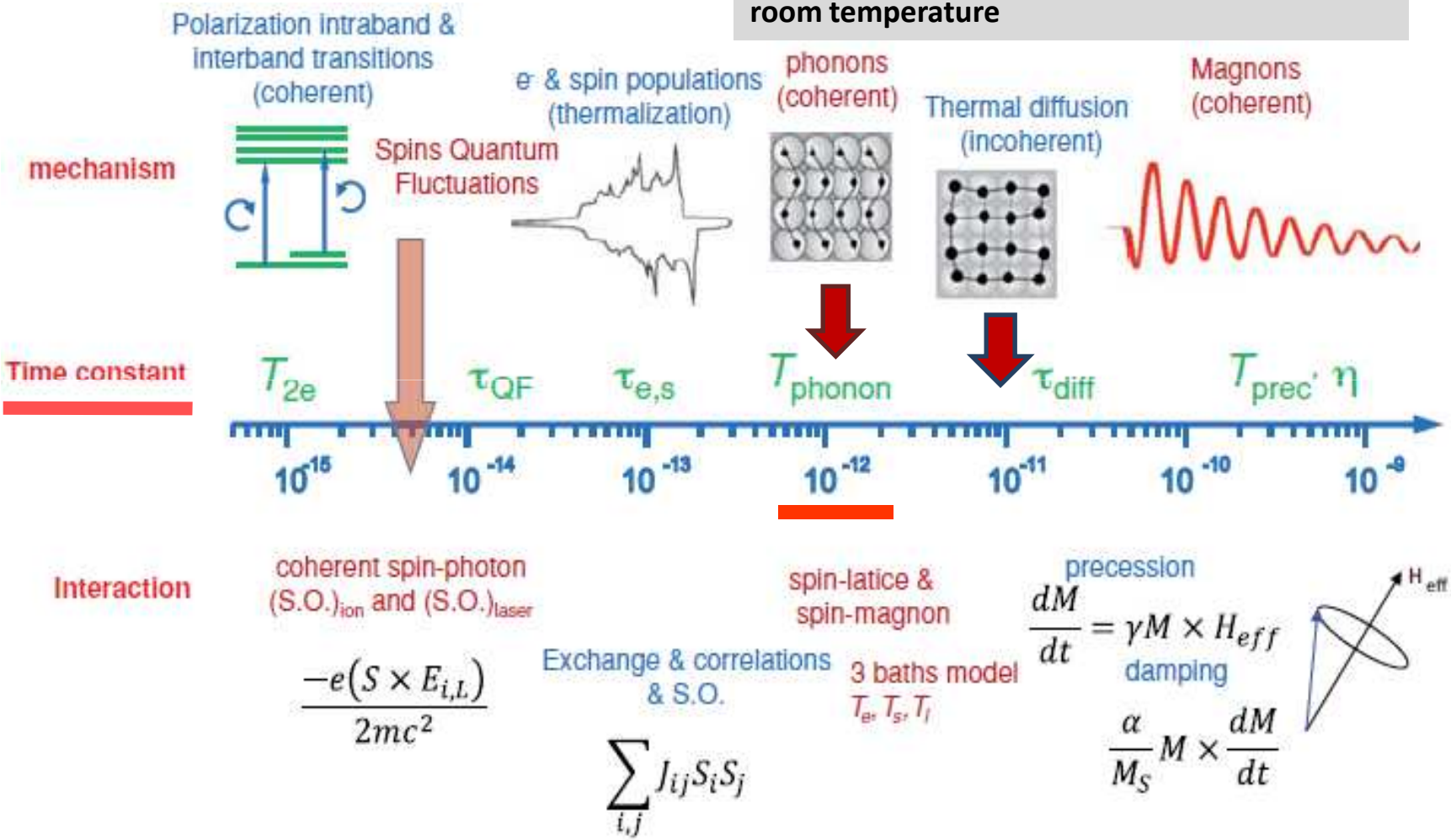

Bigot and Vomir, Ann. Phys. (Berlin) **525**, 2 (2013)

Phonon dispersion of cristalline Silicon (*Si*) at room temperature along different directions of *q* wavevectors in the 1st Brillouin zone

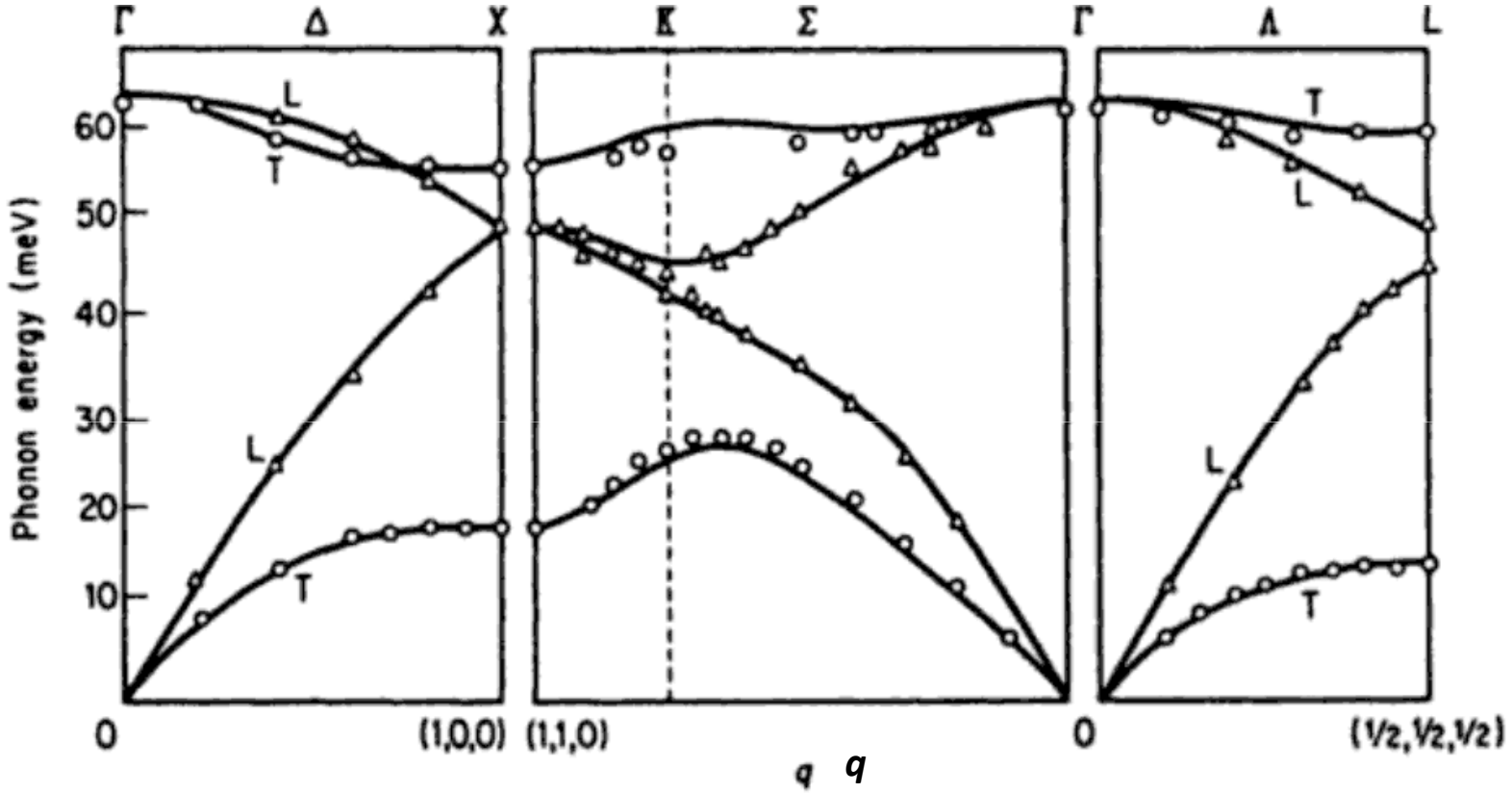

Measured phonon dispersion for *Si* with *q* units of $2\pi/a$, where *a* is the lattice parameter of the unit cell.

1 THz = 4.1357 meV = 33.356 cm^{-1}

Dolling (1963);
reproduced from *Elliot and Gibson* (1982)

Phonon dispersion of the solidified fcc crystalline Neon (*Ne*, rare gaz) at 4.7 K temperature, along different *q* directions in the 1st Brillouin zone

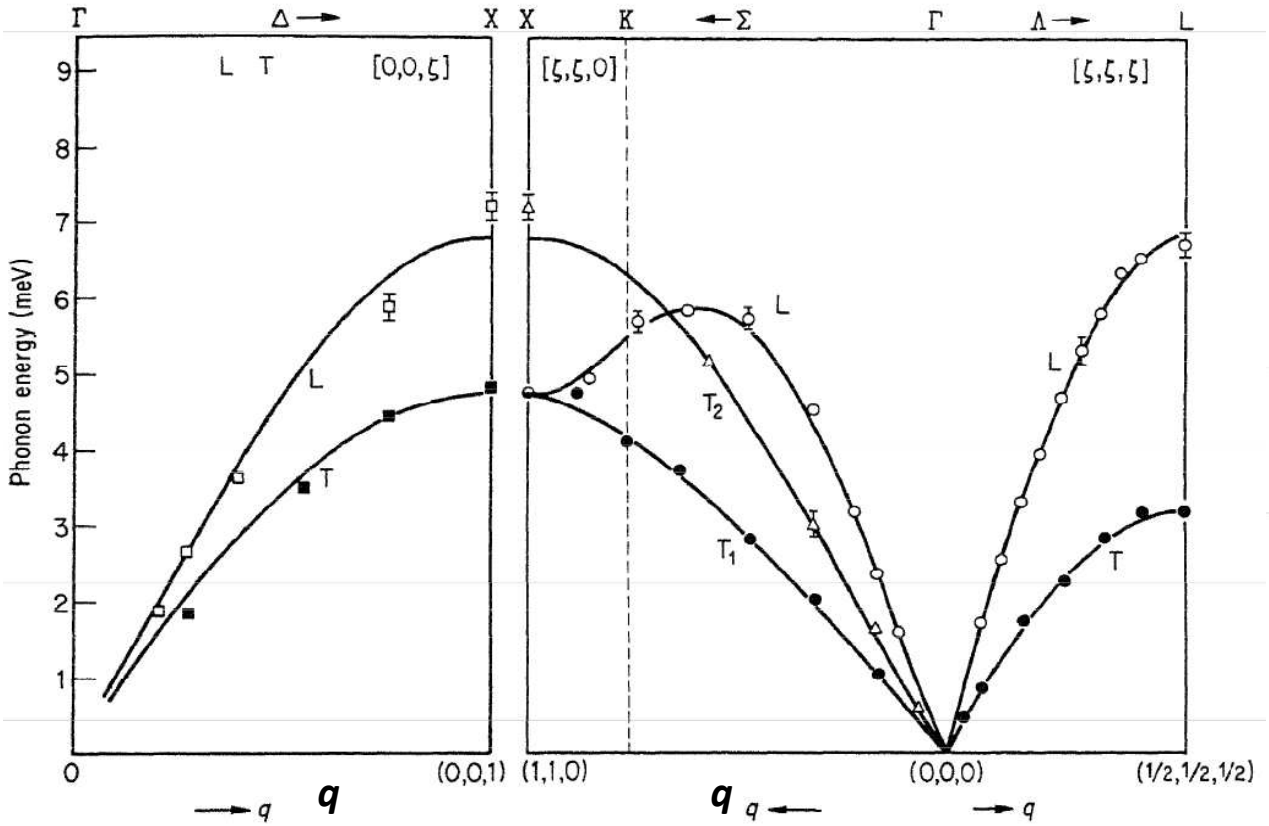

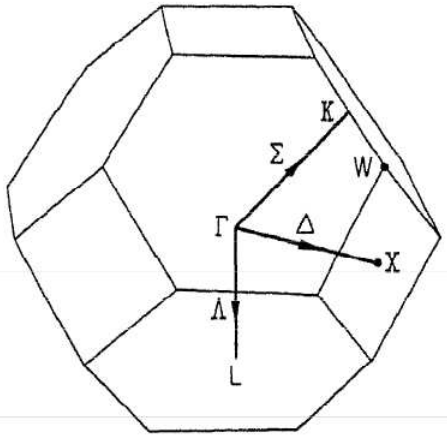

The **1st Brillouin zone** of the planes (100), (110), and (111) of a **fcc crystal**

Measured phonon dispersion in the solid cristalline fcc *Ne* at 4.7 K, *q* in units of $2\pi/a$, where *a* is the lattice parameter

Leak et al (1969);
reproduced from *Elliot and Gibson* (1982)

Phononics at the lower end of the Nanoscale ~ 1 nano

The vibration dynamics in phononics at the atomic scale, for stable crystalline nanostructures

Phononic thermal conductance in 2D systems across an integrated nanostructure

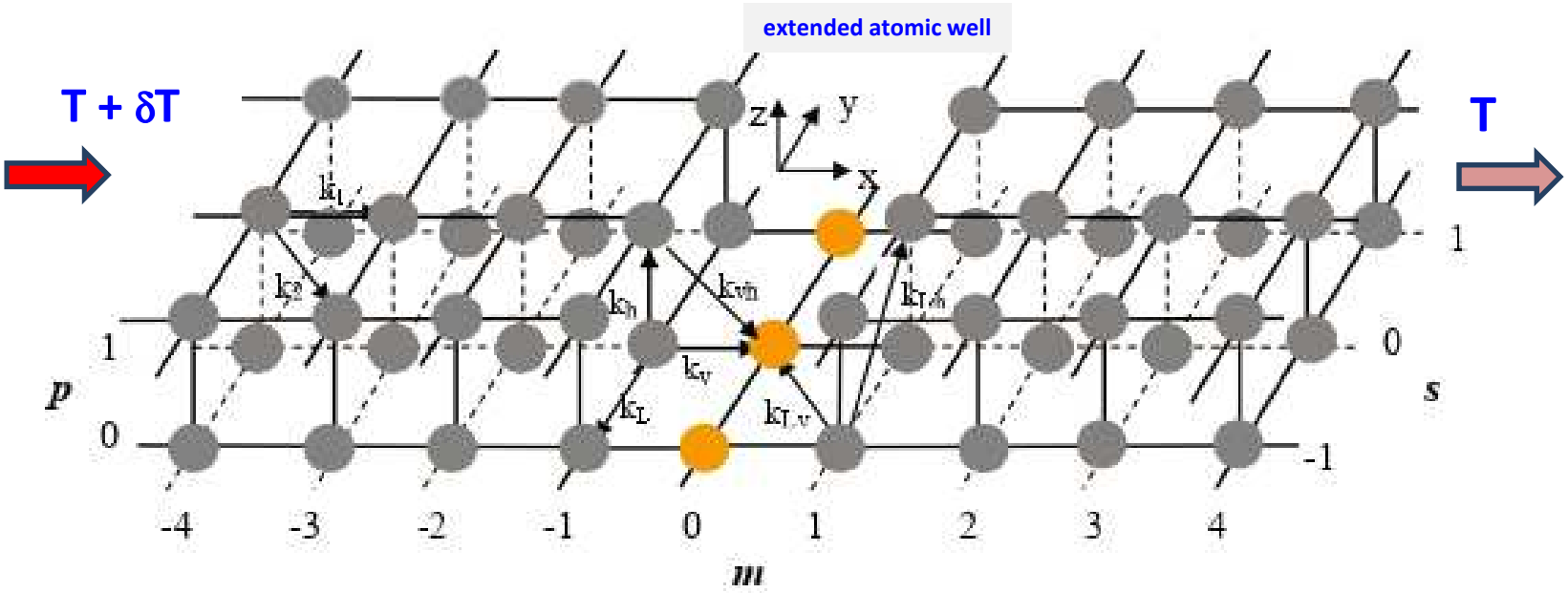

Schematic figure for ultrathin crystalline Gold (*Au*) film of two semi-infinite atomic layers, with an extended atomic well integrated nanostructure. The *y* axis is parallel to the well along the colour online, and *z* axis normal to the film.

1st and 2nd nearest neighbours force constants, *ab initio* computations : k_1=56 Nm^{-1} and k_2=7.56 Nm^{-1}

Khater et al, Eur. Phys J. B **80**, 363 (2011)

Wu et al, Phys. Rev. B **67,** 134103 (2003)

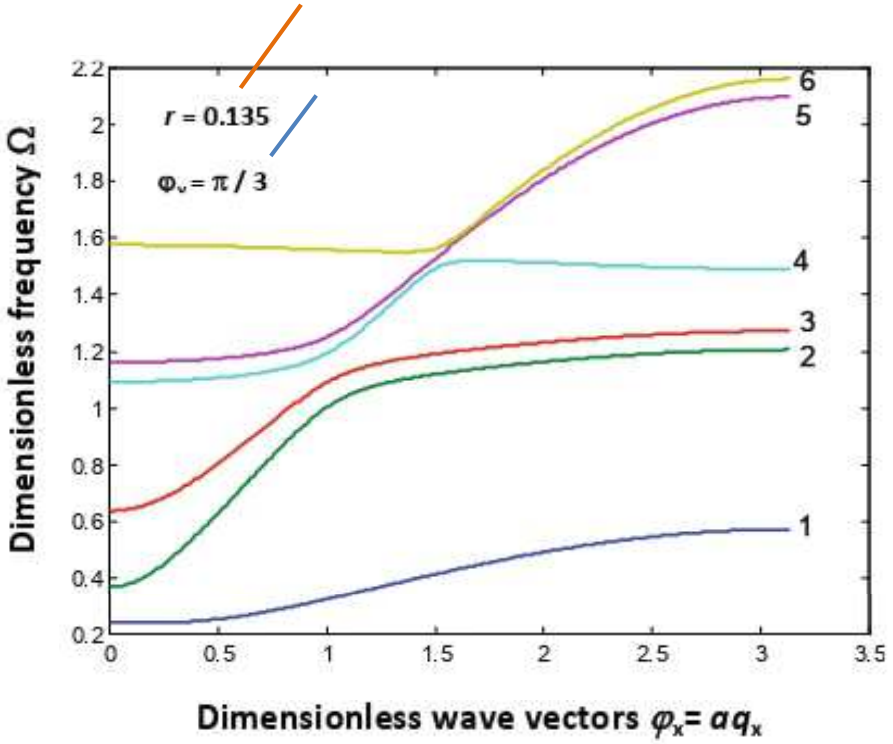

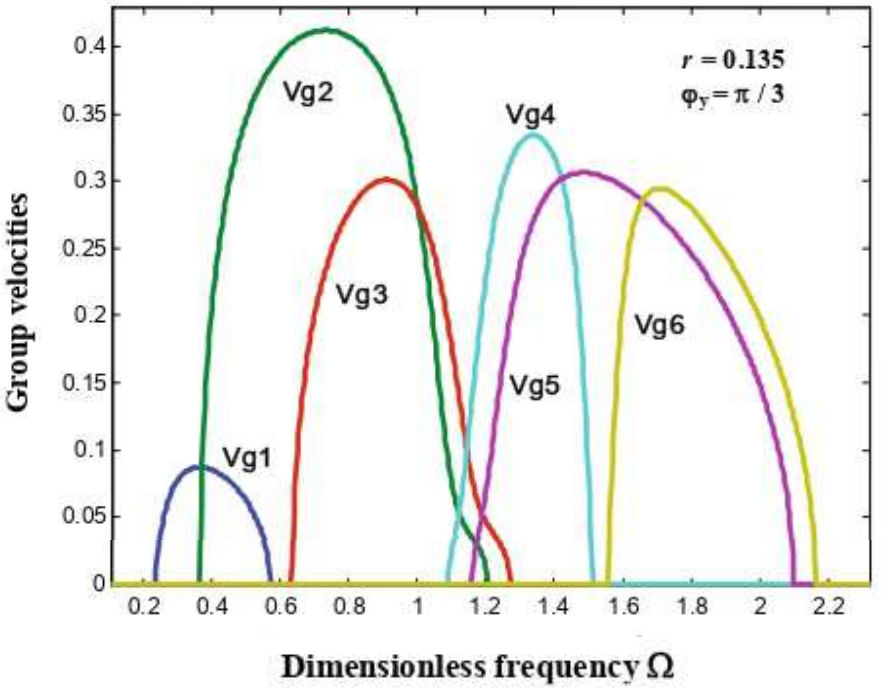

Fig. 2. (Color online) Typical phonon dispersion curves for the ultrathin Au films are presented over the BZ, $\varphi_x = [-\pi, \pi]$, for a chosen component $\varphi_y = \pi/3$ of the dimensionless wave-vector. The six available modes are indexed $j' = 1, 2, 3, 4, 5, 6$, from bottom to top.

Fig. 3. (Color online) The group velocities v_{gj} for the phonon modes in the bulk of the Au thin films as a function of the dimensionless frequencies Ω, for a chosen component $\varphi_y = \pi/3$ of the dimensionless wave-vector.

1st and 2nd nearest neighbours *ab initio* force constants k_1=56 Nm^{-1} and k_2=7.56 Nm^{-1} ; $r = k_2/k_1$

$\Omega = \omega/\omega_0$

ω_0 = 54 meV = 13.04 THz

Phase Field Matching Theory (PFT) method computes the **Transmission Probability** t of the ***j'*** **.th phonon mode** incident from a lead, across a nanostructure

The ensemble of lead phonons { *j* } , whether propagating or evanescent, should be considered

Consider an incident lead phonon *j'* which scatters at the nanostructure into transmitted and reflected { *j* } phonons

$T_{j,j'}$ Transmission *amplitude* of *j*

$R_{j,j'}$ Reflection *amplitude* of *j*

For the complete description of the reflection and transmission processes, calculate the Reflection and Transmission Probabilities: given respectively by

$$t_{j,j'}(\varphi_y,\Omega)=\frac{v_{gj}}{v_{gj'}}|T_{j,j'}|^2$$
$$r_{j,j'}(\varphi_y,\Omega)=\frac{v_{gj}}{v_{gj'}}|R_{j,j'}|^2.$$

$$t_{j'}(\varphi_y,\Omega)=\sum_j t_{j,j'}(\varphi_y,\Omega)$$
$$r_{j'}(\varphi_y,\Omega)=\sum_j r_{j,j'}(\varphi_y,\Omega).$$

$$t_{j'}(\varphi_y,\Omega)+r_{j'}(\varphi_y,\Omega)=1.$$

v_{gj} is the group velocity of the corresponding phonons

Method to compute the Phononics Thermal Conductance across nanostructures and interfaces

$$\frac{1}{a^r sd} Q_{i,T+\Delta T} = \frac{1}{a^{r-1} sd} \int d\boldsymbol{q}\, \hbar\omega_i(q, q_z)\, \frac{1}{a} \frac{\partial \omega_i(\boldsymbol{q}, q_z)}{\partial q_z}\, \boldsymbol{t}(\omega_i(\boldsymbol{q}, q_z))\, \frac{1}{e^{\hbar\omega_i/k_B(T+\Delta T)} - 1}$$

$$= \frac{1}{a^{r-1} sd} \int d\boldsymbol{\varphi}\, \hbar\, [\,\omega_0]^2\, \Omega_i(\boldsymbol{\varphi}, \varphi_z)\, \frac{\partial \Omega_i(\boldsymbol{\varphi}, \varphi_z)}{\partial \varphi_z}\, \boldsymbol{t}(\Omega_i(\boldsymbol{\varphi}, \varphi_z))\, \frac{1}{e^{\hbar\Omega_i/k_B(T+\Delta T)} - 1}$$

$\boldsymbol{K_i} \equiv \boldsymbol{K}$ (*mode i*) is the **Thermal Conductance, across a nanostructure, for the *i.* th lead phonon**

$$\kappa(mode\ i\ ) = Lt\ \Delta T \to 0\ \ \frac{1}{a^r sd} \frac{[Q_{i,T+\delta T} - Q_{i,T}]}{\Delta T} = \frac{1}{a^r sd} \frac{\partial Q_{i,T}}{\partial T}$$

$$= \frac{k_B \omega_0}{a^{r-1} sd} \int d\boldsymbol{\varphi}\, \left[\frac{\hbar\omega_0}{k_B T}\right]^2\, \Omega_i{}^2(\boldsymbol{\varphi}, \varphi_z)\, \frac{\partial \Omega_i(\boldsymbol{\varphi}, \varphi_z)}{\partial \varphi_z}\, \boldsymbol{t}(\Omega_i(\boldsymbol{\varphi}, \varphi_z))\, \frac{e^{\hbar\omega_0\Omega_i/k_B T}}{[e^{\hbar\omega_0\Omega_i/k_B T} - 1]^2}$$

where $\boldsymbol{t}(\Omega_i)$ is the **Transmission Probability, across the nanostructure, for the *i.* th lead phonon**

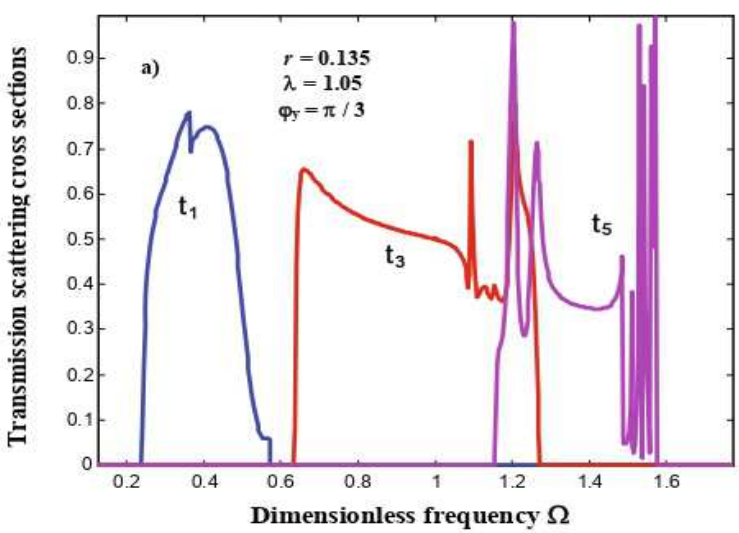

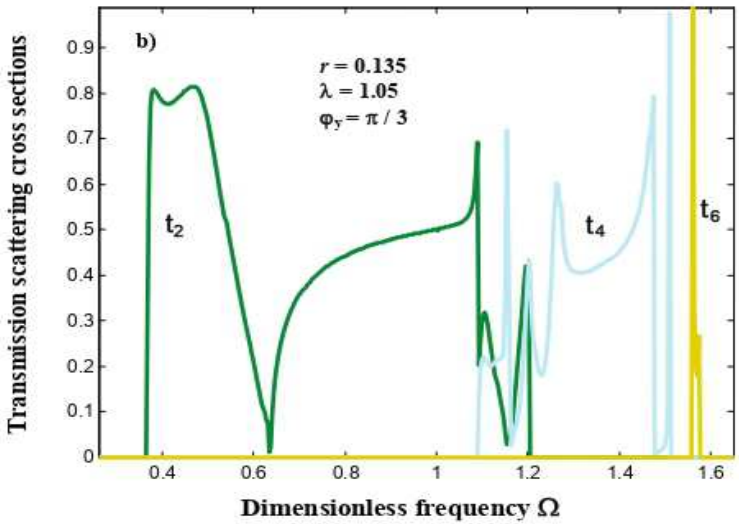

Fig. 4. (Color online) (a) The transmission scattering spectra for the atomic well boundary in the Au thin films system, presented as a function of the dimensionless frequencies Ω, for the odd numbered phonon eigenmodes, for a chosen component $\varphi_y = \pi/3$ of the dimensionless wave-vector, and under boundary *hardening* $\lambda = 1.05$. (b) as in (a) for the even numbered phonon eigenmodes.

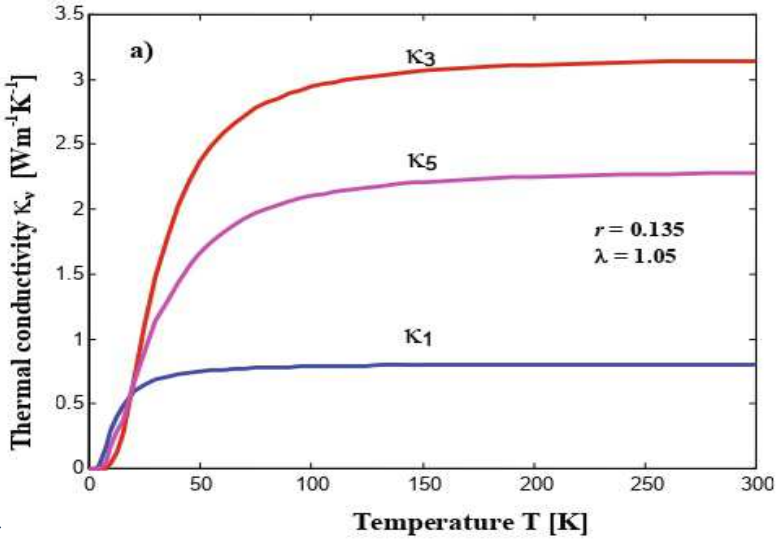

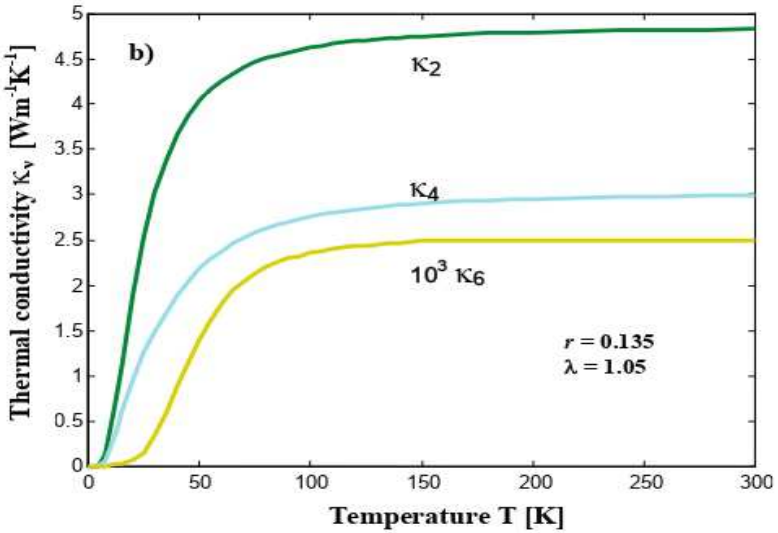

Fig. 6. (Color online) The phonon coherent thermal conductivities $\kappa_{j'}$ as a function of the temperature, at the Au atomic well boundary, for the even numbered phonon modes, under boundary *hardening* $\lambda = 1.05$. (b) as in (a) for the even numbered phonon modes.

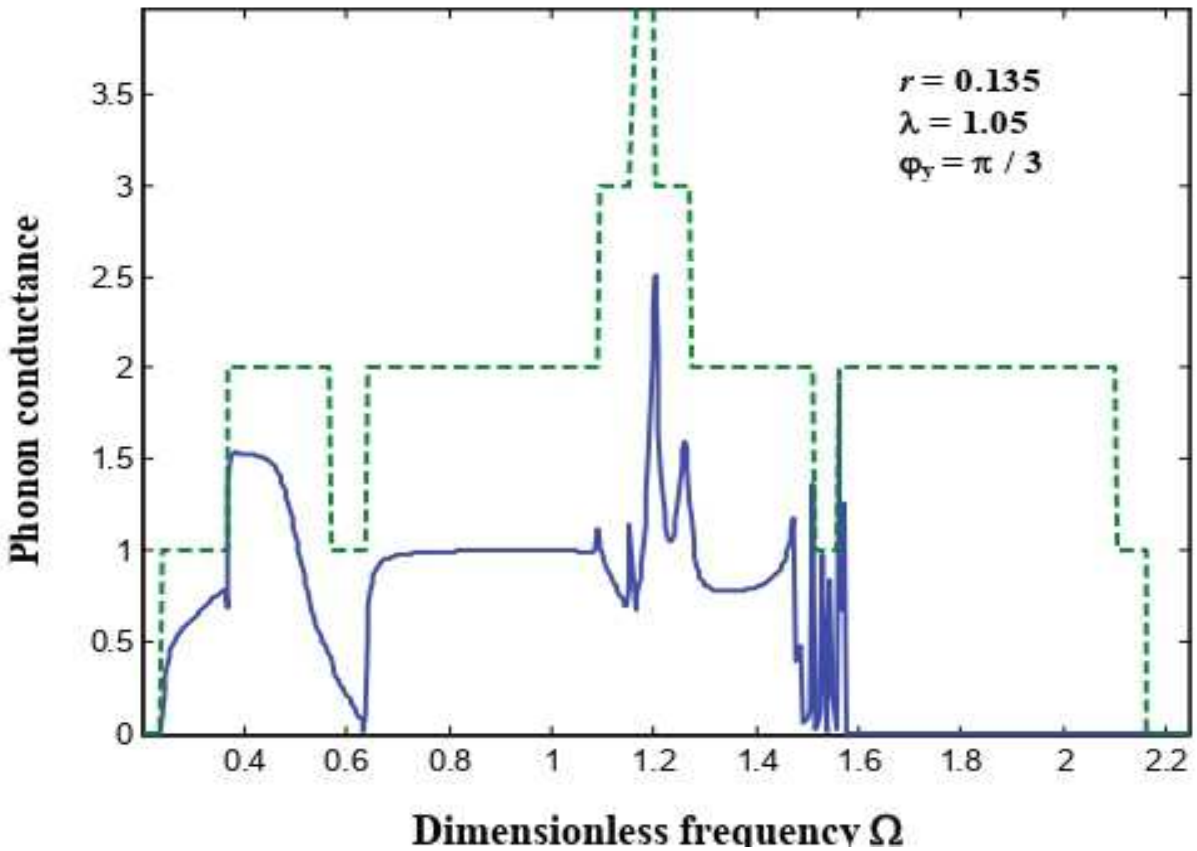

The total spectral conductance, across the *Au* nanostructured atomic well, between 2D film layers, for phonons incident at a $\varphi_y = \pi/3$ angle

PFMT theory for the phonon ballistic thermal transport on gold nanowires across topological nanostructures

Gold (*Au*) nanowire with a topological nanostructure

The gray rectangle indicates the considered nanostructure

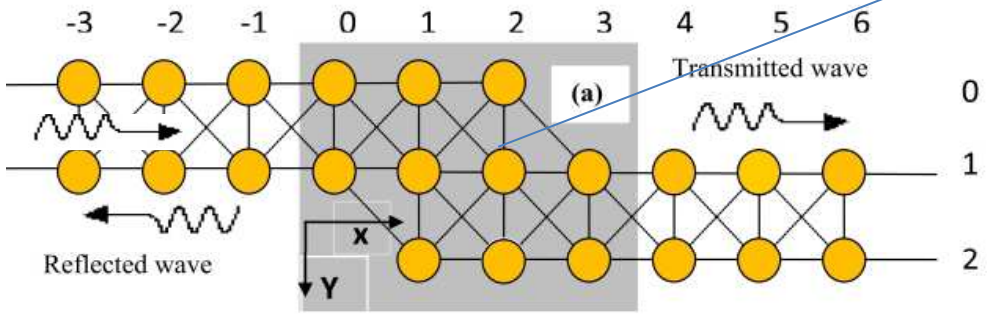

The topological nanostructure is in the form of an L bend along the *Au* nanowire.
The primitive unit cell is of 2 atoms along Y in the XY plane, with two vibration degrees of freedom

1st and 2nd nearest neighbour force constants of *ab initio* computations : k_1=56 Nm^{-1} and k_2=7.56 Nm^{-1}

Wu et al, Phys. Rev. B **67,** 134103 (2003)

$$\Omega = \omega/\omega_0$$

ω_0 = 54 meV = 13.04 THz

Belhadi and Khater, Physica E **88**, 97 (2017)

Fellay et al, Phys. Rev. B **55**, 1707 (1997)

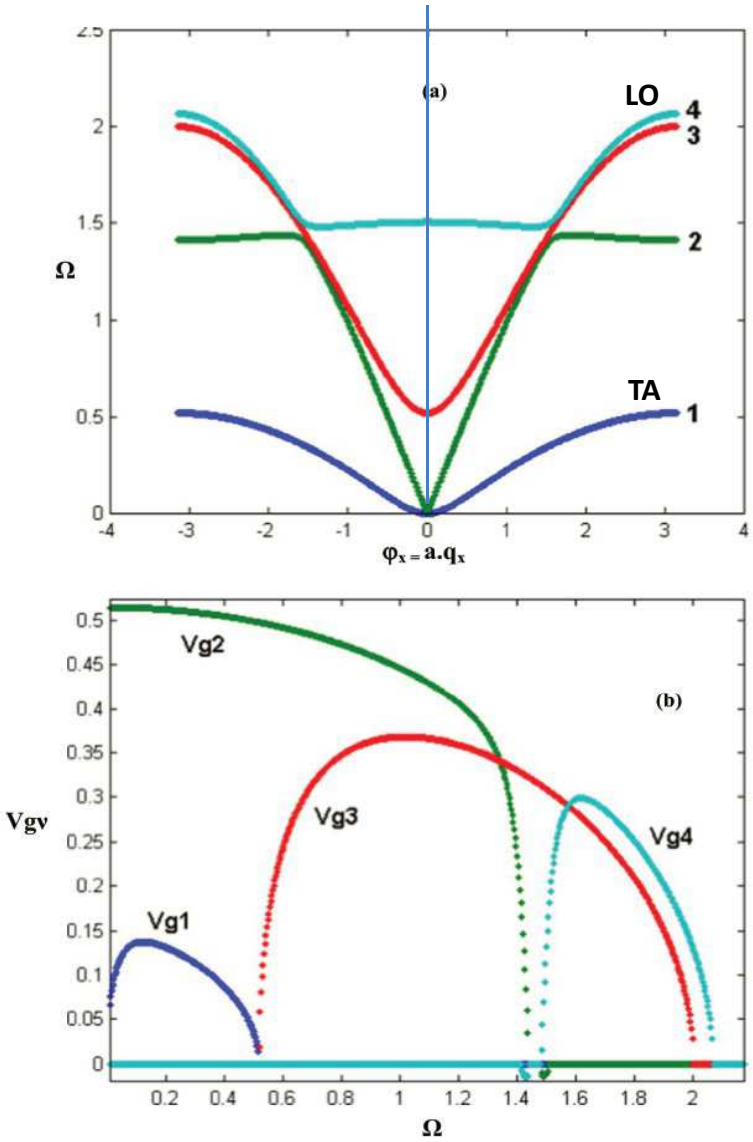

PFMT computed Transmission Probabilities

L2aL

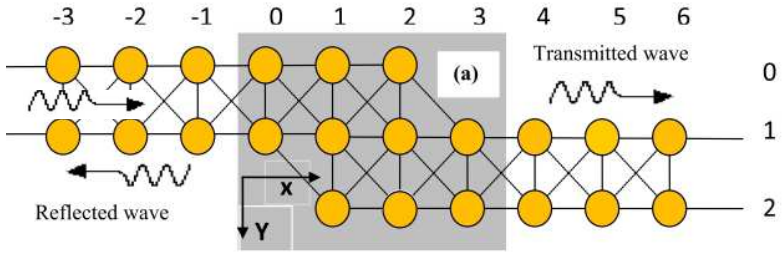

L3aL

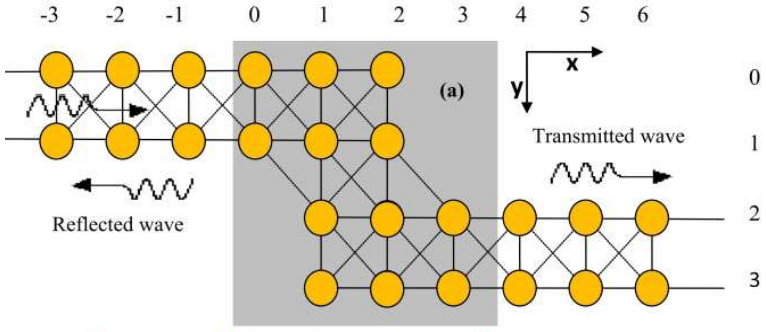

L4aL

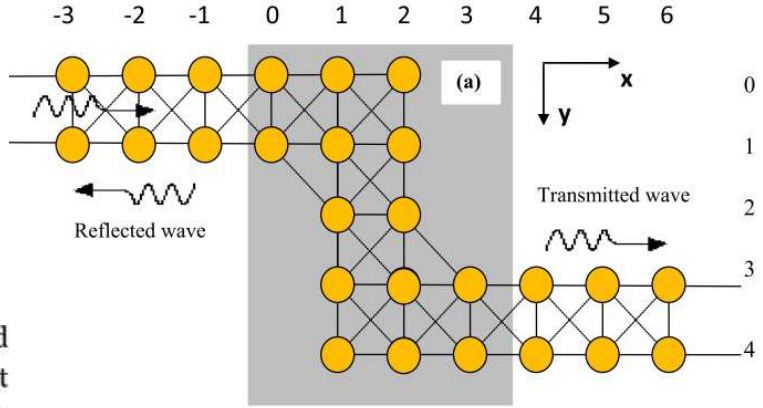

Fig. 1. (a) Typical phonon dispersion curves are given for the considered perfect Gold nanowire. The dispersion curves are shown over the interval $\varphi_x=[-\pi , +\pi]$ of the first Brillouin Zone. The modes are indexed from the bottom to top. (b) Phonon group velocity vg for confined phonon branches as a function of the dimensionless frequency Ω, in a one dimensional Gold nanowire.

The **transmission probabilities** and **phononic thermal conductance** for the **L2aL** system

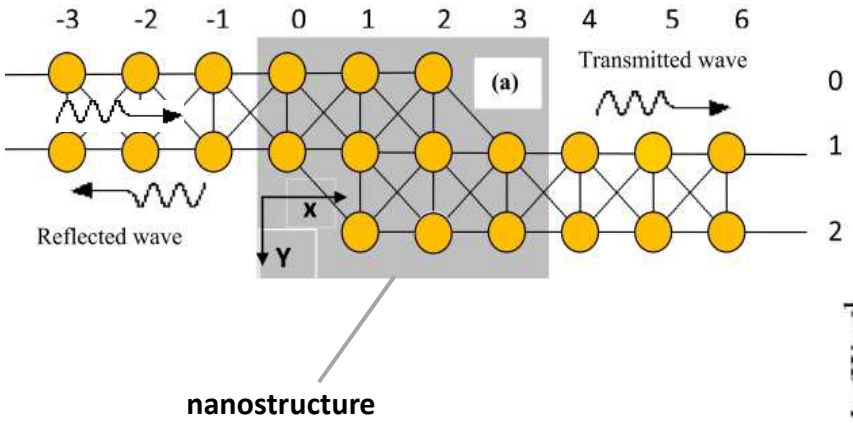

visible **Fano effects** on the **Transmission Spectra**

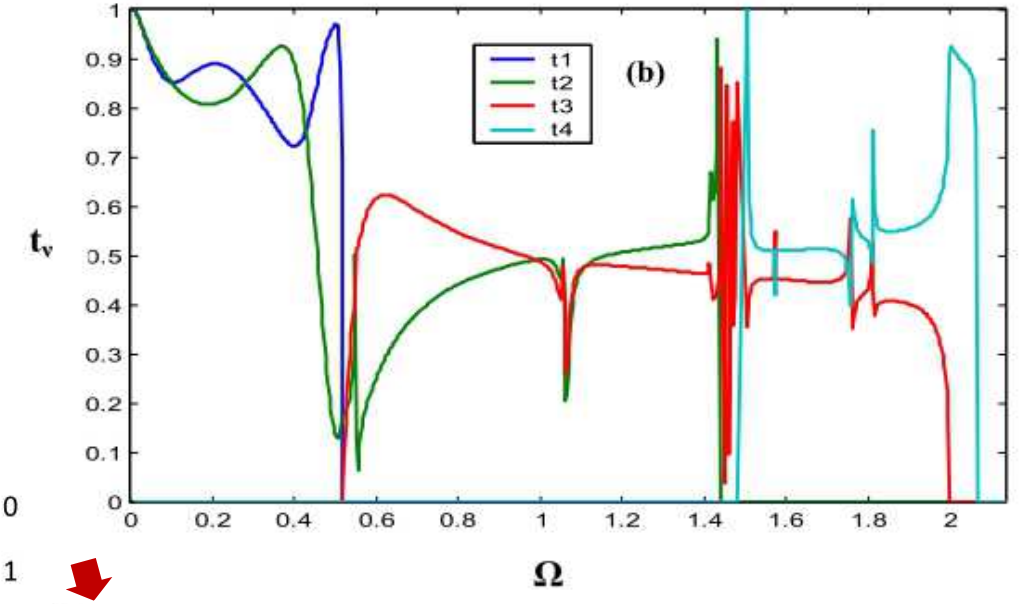

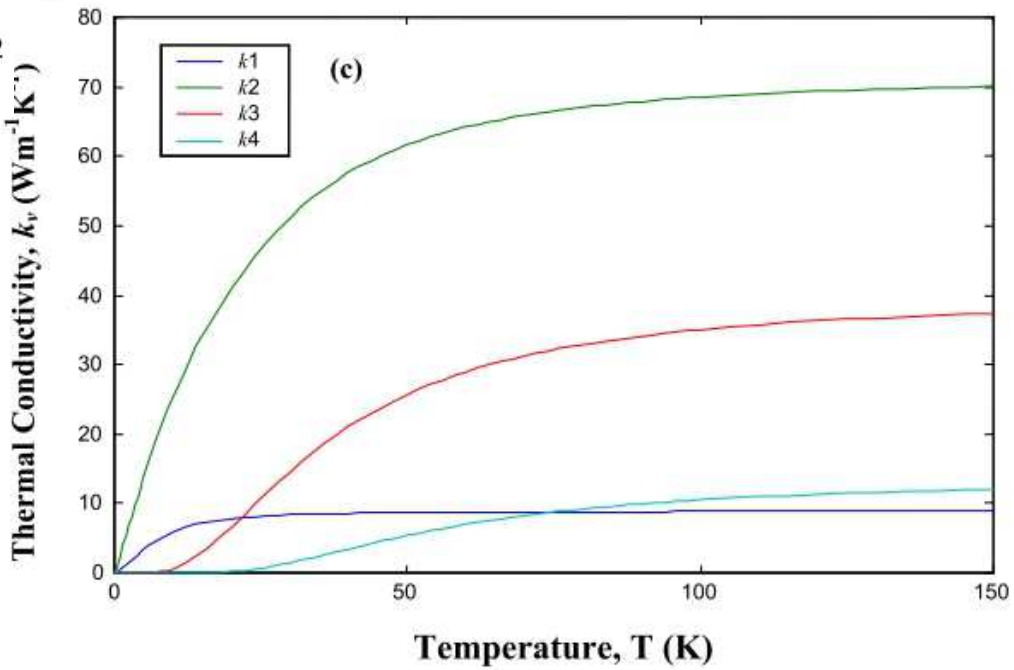

The transmission probabilities and phononic thermal conductance for the L3aL system

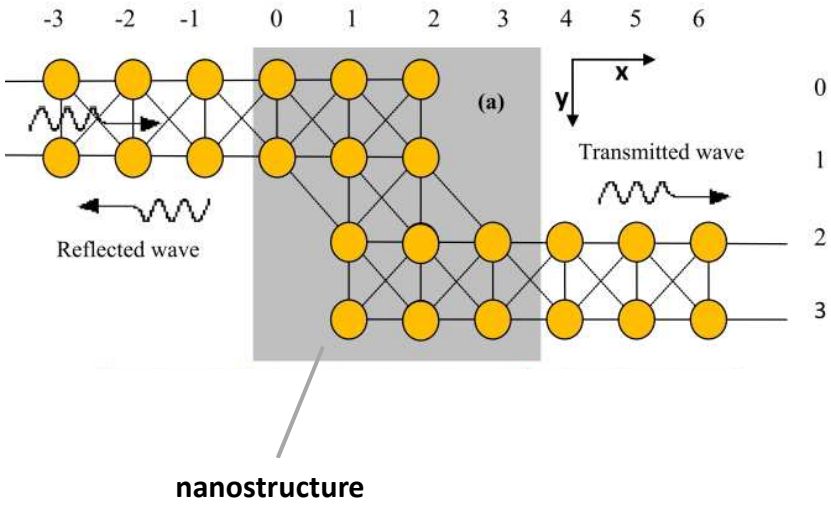

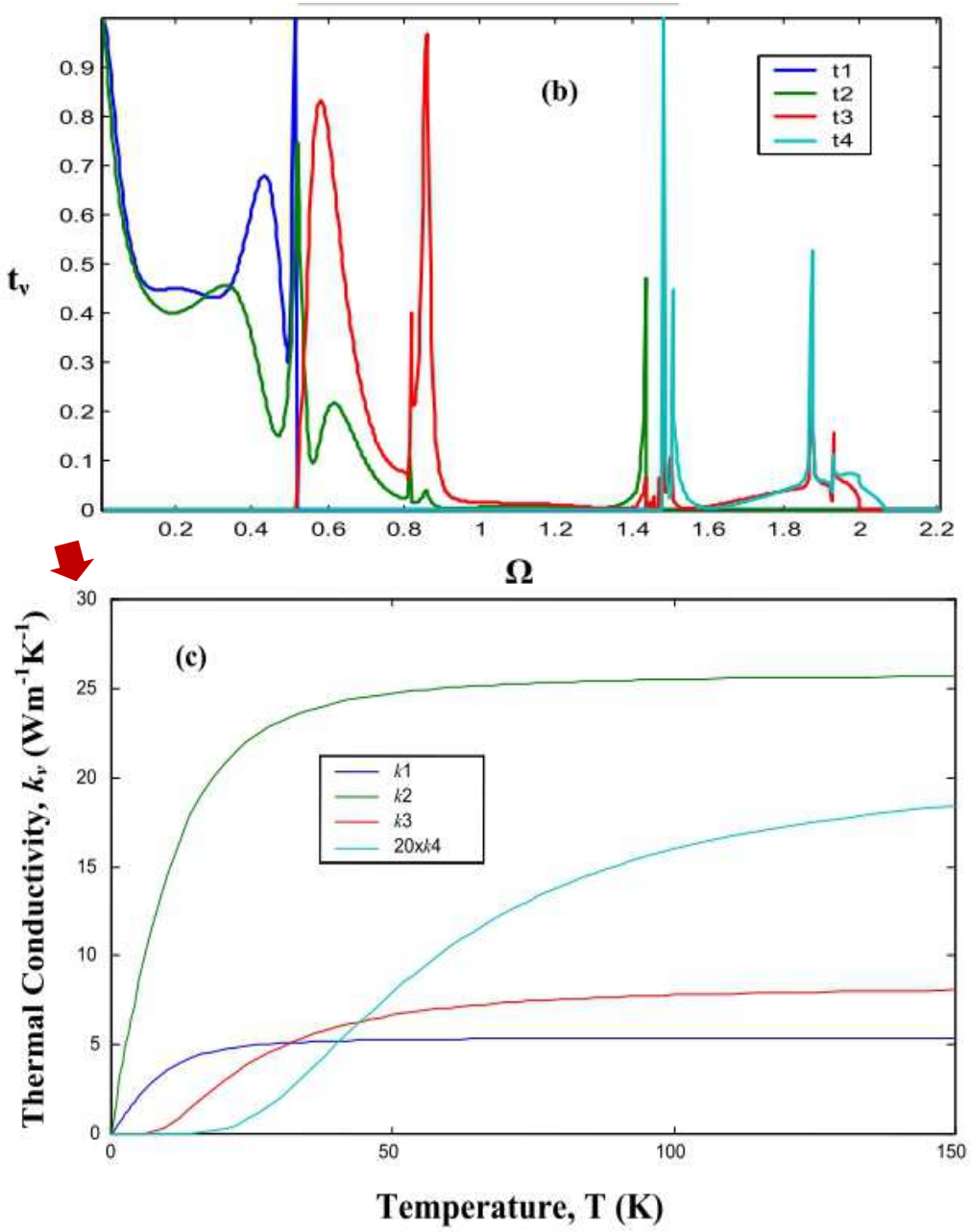

visible Fano and Fabry-Pérot effects on the Transmission Spectra

The transmission probabilities and phononic thermal conductance for the L4aL system

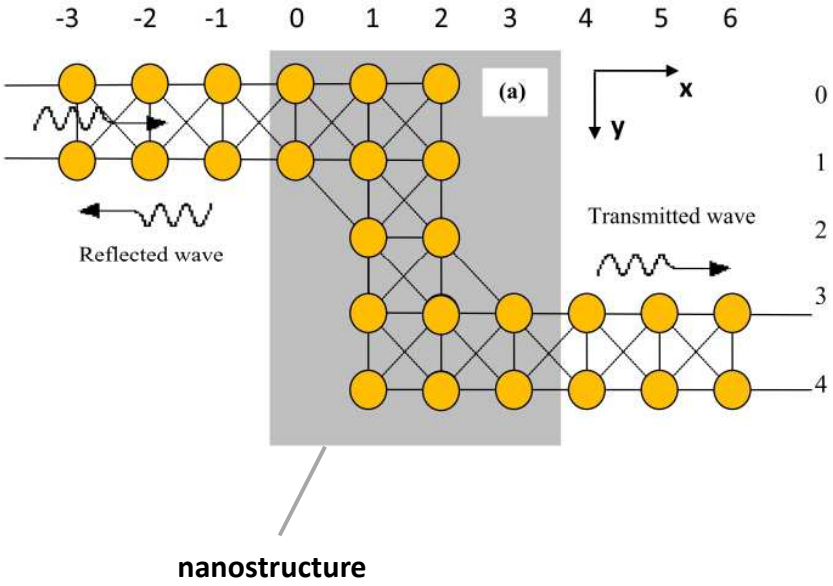

visible Fano and Fabry-Pérot effects on the Transmission Spectra

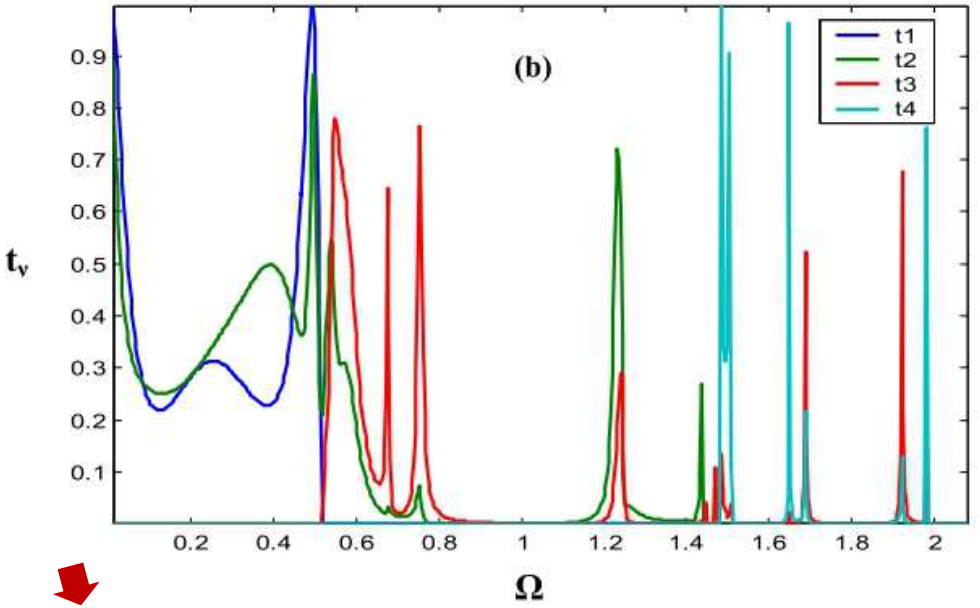

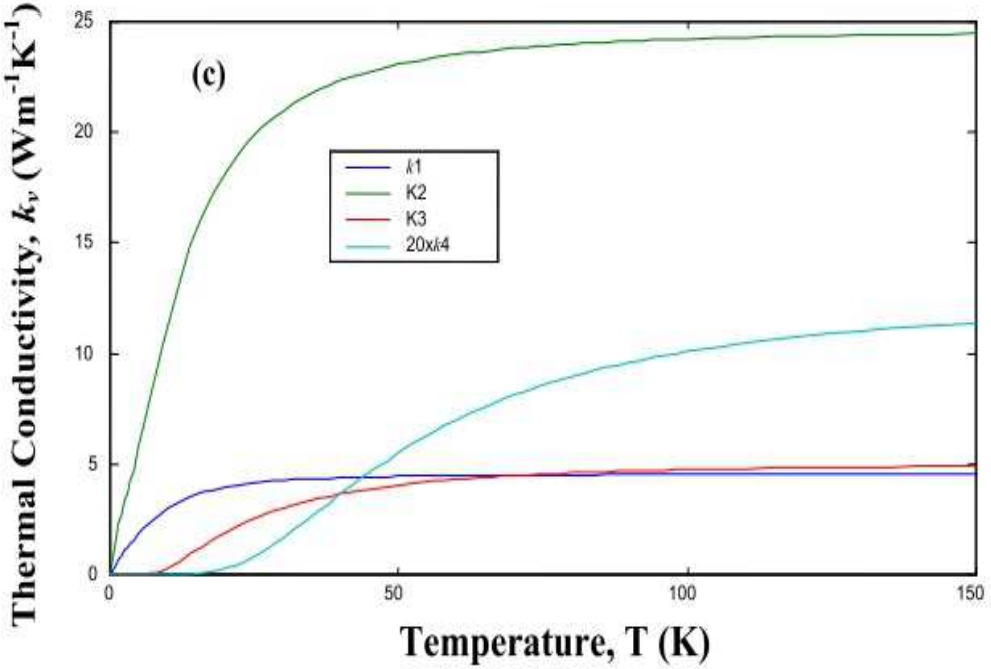

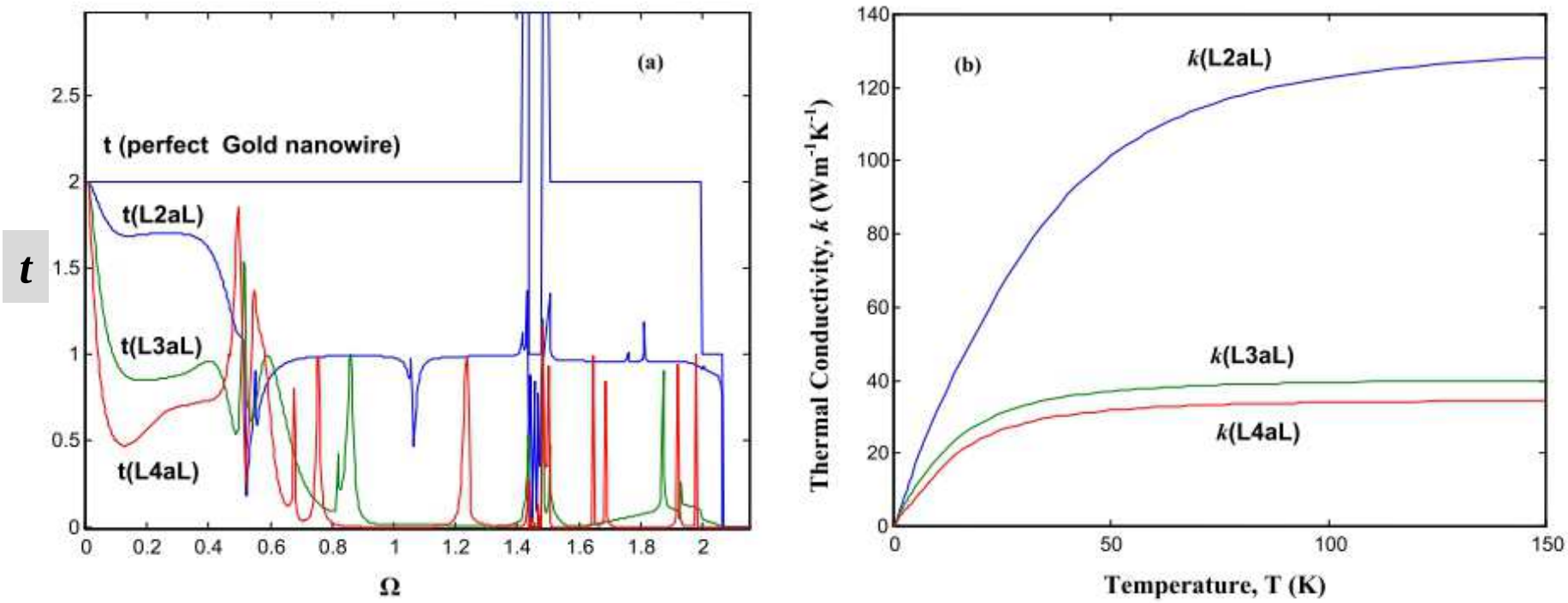

Fig. 5. (a) The total phonon conductance of the system as a function of the scattering frequency Ω for different shaped joint nanostructures width (b) Low temperature behavior of phonon thermal conductance k of the system as a function of the temperature T for different shaped joint nanostructures width.

Phononics at higher Nanoscales $\geq$ a few nanos

The continuum dynamics for isotropic and anisotropic materials

Some properties of phonons

Thermal transport in solid materials is dominated by acoustic phonons; at room-temperature the contribution of longitudinal phonons is only ~ 3%

G.P. Srivastava, The Physics of Phonons (CRC Press 2023)

Acoustic phonons of relatively long lifetimes, travel over distances of 10 to 100 nm as their wave vectors go from 0.3 $Å^{-1}$ (λ ~ 2.1 nm) to 0.1 $Å^{-1}$ (λ ~ 6.3 nm)

Lory et al, Nature Communications **vol. 8**, article 491 (2017)

Gold-Parker et al, PNAS **115** (47), 11905 (2018)

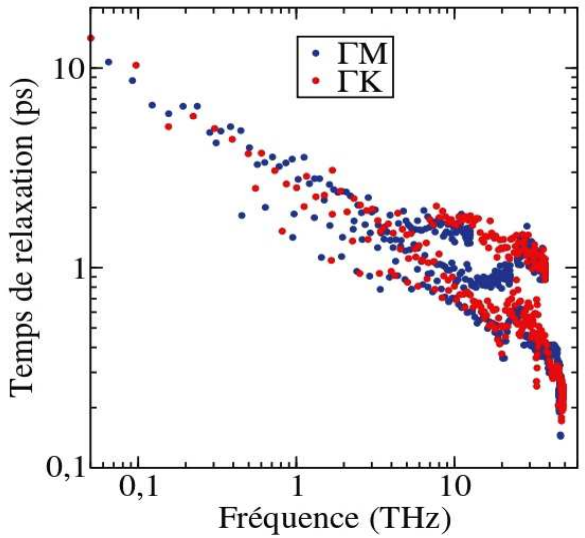

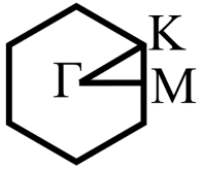

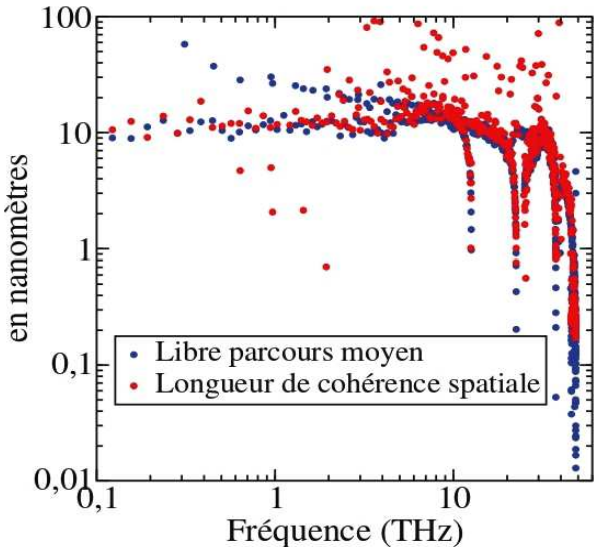

Life-time of phonons of 2D graphene, propagating along ΓM ● and ΓK ●

Comparing mean free paths ● , and spatial correlation lengths ●, for phonons of 2D graphene, along ΓM

Latour, PhD thesis at U. Paris-Saclay & Centrale Supélec 2017

Kapitza thermal conductance

schematic figure of the ballistic and diffusive channels for the transport of energy from a solid to liquid Helium

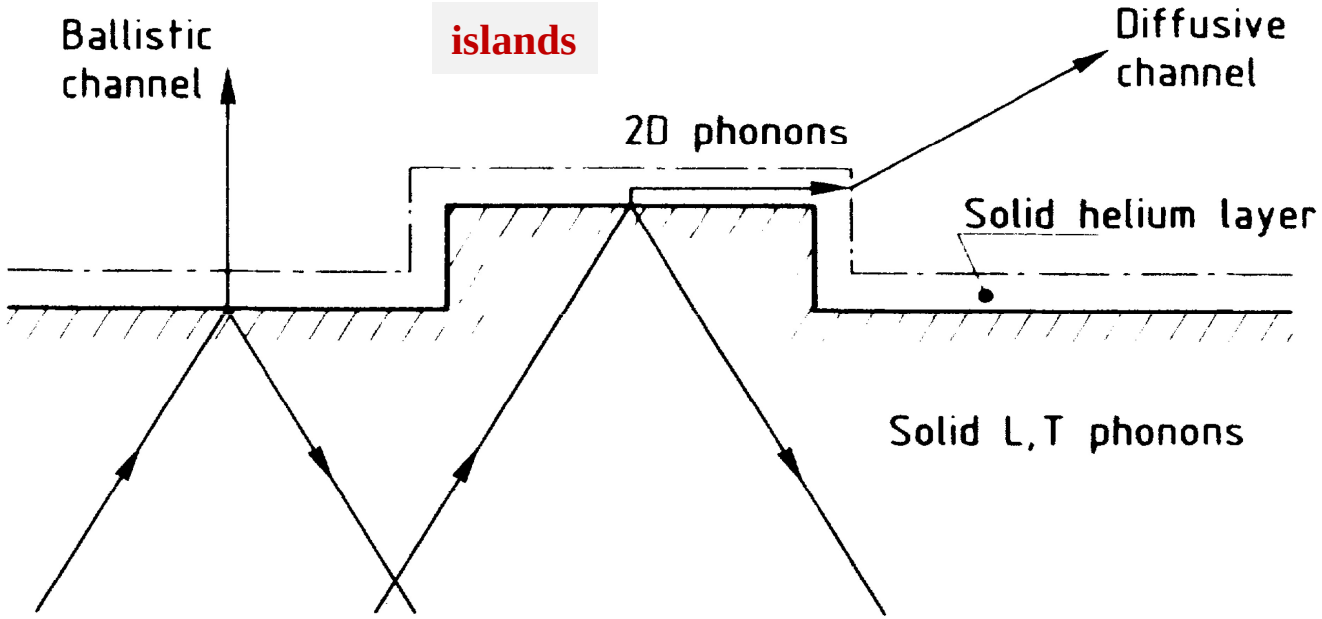

The diffusive channel is related to the elastic dynamics of irregularities at the interface solid surface – liquid He. These may be modelled as cylindrical islands of different sizes.

Khater and Szeftel, Phys. Rev. **B 35**, 6749 (1987)

Scattering of elastic waves at the plane surface of a half-space isotropic material

The dynamics of solid matter as continuous media are based on the Theory of Elasticity

Landau & Lifshitz, Theory of Elasticity (Oxford 1970)

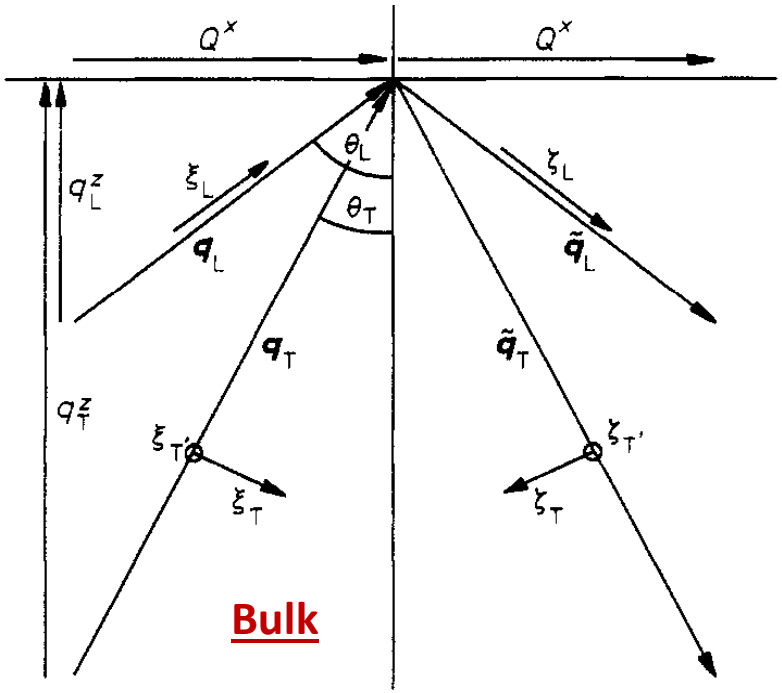

wave vectors and polarisation vectors of the incident & reflected waves on the idealized flat surface of the isotropic material.

The reflection of longitudinal & transverse waves at the plane surface of an isotropic material are calculated by surface elastic boundary conditions:

$$u_L = \Gamma_{LL} u_L^0 + \Gamma_{LT} u_T^0$$
$$u_T = \Gamma_{TL} u_L^0 + \Gamma_{TT} u_T^0$$
$$u_{T'} = u_{T'}^0$$

$$\Gamma_{LL} = \Gamma_{TT} = \{4v_T^4 Q^{x2} q_L^z q_T^z - (\omega^2 - 2v_T^2 Q^{x2})^2\}/D,$$
$$\Gamma_{LT}/v_T^2 q_T^z = -\Gamma_{TL}/v_L^2 q_L^z = 4v_T Q^x (\omega^2 - 2v_T^2 Q^{x2})/v_L D$$
$$D = 4v_T^4 Q^{x2} q_L^z q_T^z + (\omega^2 - 2v_T^2 Q^{x2})^2.$$

coherent phonons

$$q_T^2 = \omega^2/v_T^2$$
$$q_L^2 = \omega^2/v_L^2$$

Loudon, J. Phys. C: Solid State Phys. **11** (1978)

Green functions were derived for the displacement gradients associated with the acoustic vibrations, to establish a theory for Brillouin light surface scattering **at room temperature**

Modeling flexure dynamics of the cylindrical islands at the surface

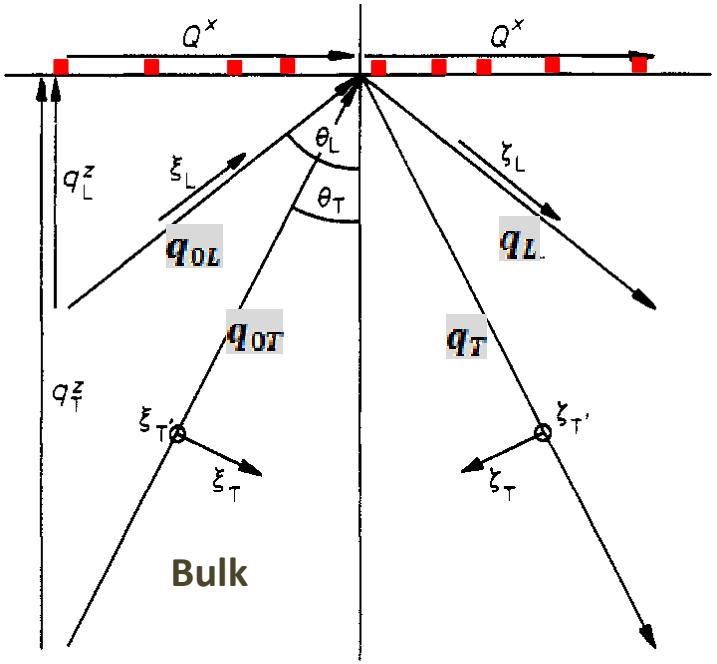

The red dots correspond to irregular islands

$$\boldsymbol{q_{0L}} = (Q^x_{0L}, 0, q^z_{0L}) \quad \boldsymbol{q_{0T}} = (Q^x_{0T}, 0, q^z_{0T})$$

$$\boldsymbol{q_L} = (Q^x_L, 0, q^z_L) \quad \boldsymbol{q_T} = (Q^x_T, 0, q^z_T)$$

$$\boldsymbol{q_T^2} = \omega^2/v_T^2 \quad \boldsymbol{q_L^2} = \omega^2/v_L^2$$

The islands have a degree of freedom of elastic flexure about the z axis, absent in a flat surface.

U_F denotes the flexure displacement amplitude. It can be calculated by the island elastic boundary conditions

$$-i\frac{\partial U_F}{\partial z}\Big|_{z=\zeta} \equiv \Gamma^r_{FL}\, U_{0L} + \Gamma^r_{FT}\, U_{0T} \equiv$$

$$\{-Aq^{z^2}_{0L} - BQ^{x^2}_{0L} - 2q^z_{0L}\,Q^x_{0L}\}\frac{v_L}{\omega}\,U_{0L}\exp[iq^z_{0L}\,\zeta] +$$

$$\{+Aq^z_{0T}\,Q^x_{0T} - Bq^z_{0T}\,Q^x_{0T} + (Q^{x^2}_{0T} - q^{z^2}_{0T})\}\frac{v_T}{\omega}\,U_{0T}\exp[iq^z_{0T}\,\zeta]$$

$$\begin{cases} A = (Q^{x^2}_L\,Q^{x^2}_T - Q^{x^2}_L\,q^{z^2}_T + 2Q^x_L\,Q^x_T\,q^z_L\,q^z_T)/Q^x_T\,q^z_T\,, \\ B = (-q^{z^2}_L\,Q^{x^2}_T + q^{z^2}_L\,q^{z^2}_T + 2Q^x_L\,Q^x_T\,q^z_L\,q^z_T)/Q^x_T\,q^z_T\,. \end{cases}$$

Khater, Europhysics Letters **2**, 539 (1986)

Island flexure dynamics excited by scattering bulk phonons at the surface

At low temperatures [0.01° - 2° K] of Kapitza conductance experiments, the *T* phonons are predominant over *L* phonons, as carriers of the elastic energy in the solid.

***T* phonons induce the harmonic flexure at the free surfaces of the cylindrical islands :**

$$u'_F \mid_{z=\zeta} = 2\frac{\omega}{v_T}\cos(2\alpha)u_{0T}e^{-i\pi/2}e^{iq^z_{0T}\zeta}e^{-i\omega t}$$

$$\alpha = \sin^{-1}(Q^x_{0T}v_T/\omega)$$

denotes the angle of incidence of the *T* bulk phonons.

The equation of flexure dynamics of the circular islands is well known

$$\frac{\partial^2 u_F}{\partial t^2} + \frac{(1-\nu)EI_\xi}{\rho A_\xi}\frac{\partial^4 u_F}{\partial z^4} = 0$$

E and ν are, respectively, the Young's modulus of elasticity and Poisson's ratio, of the solid. I_ξ denotes the moment of area of the islands about their neutral axes. These quantities are well known in the theory of flexure of one-dimensional rods. A_ξ are the cross sectional areas of the islands.

The strain energy $W(\xi,\zeta)$ of flexure calculated for cylindrical islands, with boundary conditions at $z = 0$, and the variable heights $z = \zeta$, and radii ξ, is

$$W(\xi,\zeta) = 4\frac{A_\xi}{V}p_\xi^4 v_T^2 \zeta^3 \cos^2(2\alpha)\hbar\omega$$

$$p_\xi = [\rho A_\xi/(1-\nu)EI_\xi]^{1/4}$$

incident phonon energy **angle of incidence**

The partition of energy for the diffusive channel

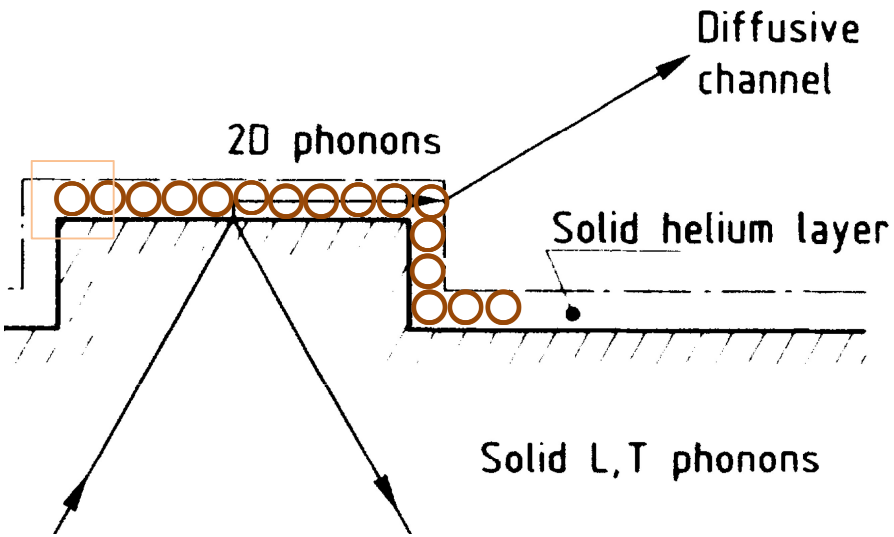

The **solid He layer** of atomic **width *d*** is attached to the island surface by **van der Waal forces.**

The **partition** of the **flexure energy** between the **island,** and the **solid He layer**, yields W_h

$$W_h = \left[\frac{1}{\xi} + \frac{8}{\xi}\right] d \frac{E'}{E} W(\xi, \xi)$$

NB: The Young modulas of elasticity for the solid He layer is $E' << E$ of the solid island

The **solid He layer** is **sandwiched** between the **island surface**, and the **surrounding liquid He**. It is **realistic to suppose** that the island harmonic flexure causes **friction-induced 2D phonons** in the He layer

The **diffusive transmission** of **dynamic energy** consists hence of the **excitation of 2D phonons** in the solid He layer and their **annihilation** via **random inelastic scattering** in the **surrounding liquid He**.

Energy transport at the solid - liquid Helium interface

The **Transmission Probability** χ_1 for phonons of $\hbar\omega$ at **incident angle** α, cross the islands involves configurational averages over their random distributions of cross sectional areas and hights.

The coefficient χ_1 is determined as

$$\chi_1(\omega,\alpha) = \frac{1}{A}\int\int N(\xi,\zeta)\,d\xi\,d\zeta\,\frac{W_h}{\tau}$$

τ is the **phonon lifetime**

$\omega\tau << 1$ at the low temperatures [0.01° - 2° K]

$$\chi_1(\omega,\alpha) = \varepsilon\beta^{-3}(1+8\beta^{-1})CE'\frac{d}{a}\cos^2(2\alpha)\hbar\omega$$

ε = surface density of islands, a solid lattice constant, β scaling for ξ and ζ, and C the **numerical product of known constant terms**.

The **heat flux** due to the flexure of the islands, at the **solid(s) - liquid He** interface can be hence determined as

$$\frac{\dot{Q}_1}{A} = \int_0^{\infty}\chi_1(\omega,\alpha)n(\omega)D(\omega)d\omega\int_0^{\pi/2}\tfrac{1}{2}v_T\sin\alpha\cos\alpha\,d\alpha$$

$$= \varepsilon\beta^{-3}(1+8\beta^{-1})CT^4E'd$$

$n(\omega)$ = phonons Bose-Einstein factor, and $D(\omega)$ the density of states of bulk phonons (its Debye model).

$$\frac{\dot{Q}_1}{A} = \varepsilon\beta^{-3}(1+8\beta^{-1})CT^4\Theta_h^2 d$$

The **value** of the **Debye temperature** Θ_h of the **solid He layer** varies with its **molar volume**, and temperature T.

Khater and Szeftel, Phys. Rev. **B 35**, 6749 (1987)

Sample and Swenson, Phys. Rev. **158**, 188 (1967)

Stewart et al, Proceedings of the 13th Int. Conference on Low Temperature Physics, pp. 180 – 185 (1974)

The thermal Kapitza resistance

The development of the theoretical model leads hence to a general analytical form for the thermal Kapitza resistance across the irregular interface of solid materials and liquid He

$$R_K T^3 = \frac{\beta^3 (1 + 8\beta^{-1})^{-1}}{2\varepsilon C d (2\Theta_h^2 + T\Theta_h \partial\Theta_h / \partial T)}$$

ε β

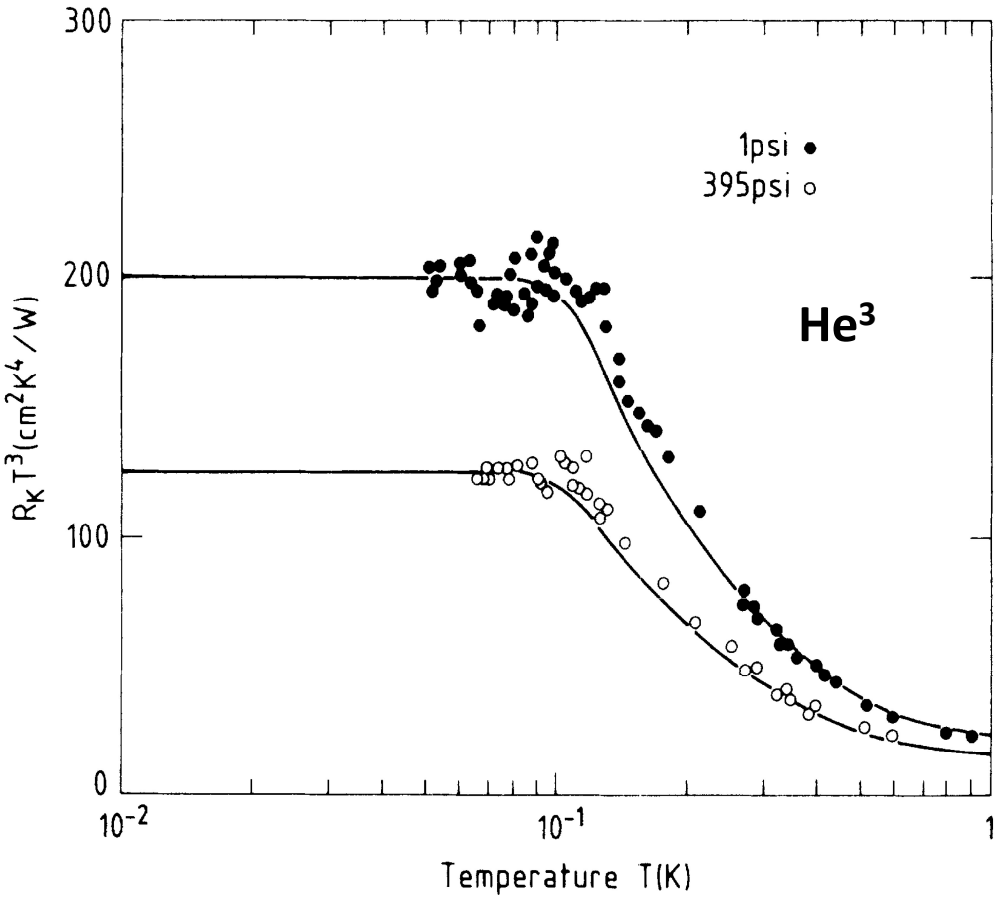

1 psi = 6894.7573 pa = 0,0680 atm
350 psi = 23,86 atm
1 pascal (pa) = 1 N/m²
1 atm = 1,013 25 bar = 101 325 pa

FIG. 2. Plots of $R_K T^3$ with temperature for a solid-liquid ^{3}He interface at two different pressures. The molar volume of the solid ^{3}He layer is 11.42 $cm^3\,mol^{-1}$. $\beta = 10$ and $\varepsilon = 1\%$. The points are the experimental measurements of Anderson *et al.* (Ref. 33). See text for details.

Phys. Rev. **135 A**, 910 (1964)

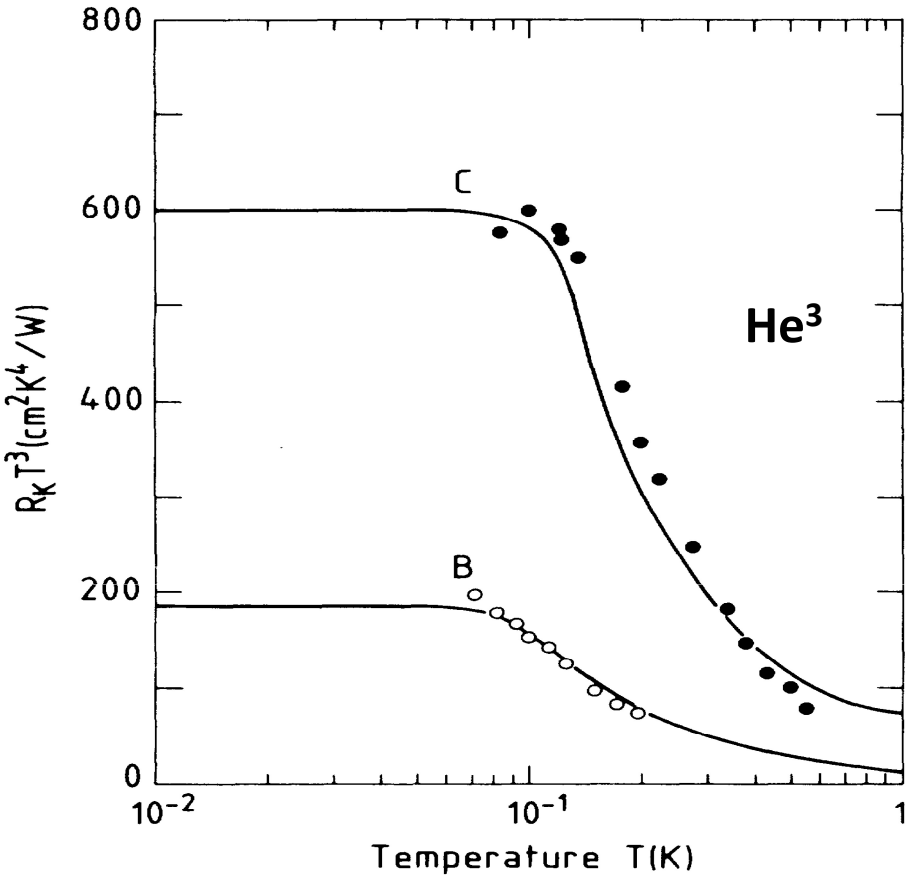

FIG. 4. Plots of $R_K T^3$ with temperature for a solid-liquid ^{3}He interface at two different surface densities of the defects, $\varepsilon = 1\%$ for curve B and $\varepsilon = 0.33\%$ for curve C; all other terms are the same as in Fig. 2. The points are the experimental measurements of Johnson and Anderson (Ref. 34). See text for details.

Phys. Lett. **37 A**, 101 (1971)

The present theory accounts for the random and bounded variation of the thermal-boundary resistance with surface preparation, since in Eq. (26) the quantities ϵ, β, and Θ_h are all random yet bounded variables. Also, the phonons emitted into helium by process (ii), assumed for the transfer mechanism in our model, have random directions consistent with the observed cosine law.[35] The theory accounts, furthermore, for the known observation that R_K is independent of the superfluidity of He II.[3] The heat flux $\dot{Q}_1/A$ calculated for the diffusive channel in Eq. (22) depends on the mechanical properties of the solid helium layer. These properties, for both solid ^{3}He and ^{4}He, are independent of the superfluid character of liquid helium.[32] The model accounts for why the heat transmission is similar for thin He films and solid He.[36] In solid He, as in the liquid under high pressures, the affected layer in which phonons are excited is larger than that in thin films.

The processes (i) and (ii) proposed for the transfer mechanism in our model can be generalized. In (i) it is sufficient to define a region of adsorbate atoms surrounding the defect where adsorbate phonons are excited by the flexure dynamics of defects. The notion of a solid adsorbate layer is not a prerequisite but the manner of variation with temperature of the elastic properties of the adsorbate atoms in this region is needed. Also, in (ii) the scattering of excited adsorbate phonons need not be limited to the scattering of 2D phonons at the step edges of the defects but may occur generally via the structural irregularities within the adsorbate films. There is evidence for such diffuse scattering,[21] with limits of a few hundred angstroms. The order of magnitude of τ, the relaxation time for process (ii) given above by Eq. (10), is unaffected by this generalization.

The transmission coefficient χ_1 for the diffusive channel obtained in approximate form in Eq. (19) varies linearly with the energy of incident phonons $\hbar\omega$. This approximation is adequate for thermal phonons from a blackbody source at low temperatures, and for defects of atomic dimensions. The detailed theory for phonon scattering in irregular surfaces[22] gives, however, physically appropriate limits for scattering when $\omega \to 0$ and $\omega \to \infty$. In these limits $q\zeta \ll 1$ and $q\zeta \gg 1$, respectively, and the corresponding phonons are shown to scatter effectively from flat surfaces without exciting flexure on the defects. χ_1 of Eq. (19) here contrasts with t_1 of Eq. (1) in Ref. 18. In Kinder's work the transmission coefficient and the model are strictly valid, provided the strain dynamics of the defects are neglected. In our work this problem is specifically investigated. The energy transmission is shown to be due to the flexure of defects in the solid surface that coherently generate phonons in the adsorbed helium layer, and to the diffusive decay of these phonons into the liquid helium bath. The energy transmission coefficient is given in general and calculated for atomically irregular surfaces. The theoretical results for the Kapitza resistance compare favorably with measurements.

ACKNOWLEDGMENTS

We should like to thank J. Tilley, and especially F. Sheard, A. F. G. Wyatt, and W. Eisenmenger for useful comments. Part of this work was done on a visit to International Centre for Theoretical Physics (ICTP), Trieste, made possible by a grant from the Royal Society of the United Kingdom and the Italian National Academy of Sciences to one of us (A.K.), and the author extends his thanks to both institutions and to T. B. Benjamin, for their support.

Develop using the two methodologies together across the Nanoscales ?

V.L. Popov, M. Heß, E. Willert
Handbook of Contact Mechanics, (Springer 2019)

J.E. Bishop and H. Lim
Continuum approximations
in *Multiscale Materials Modeling for Nanomechanics* (Springer 2016), Eds. Ch. Weinberger & G. Tucker

B. Luan and M.O. Robbins
Contact of single asperities with varying adhesion: Comparing continuum mechanics to atomistic simulations
Phys. Rev. E **74**, 026111 (2006)

R. Miller and R. Phillips
Critical analysis of local constitutive models for slip and decohesion
Philosophical Magazine A **73** (4), 803 -827 (1996)

L. Monette and M.P. Anderson
Elastic and fracture properties of the two-dimensional triangular and square lattices,
Modelling Simul. Mater. Sci. Eng. **2**, 53-66 (1994)

Yan Pennec

Doried Ghader

Boualem Bourahla

Dominik Szczęśniak

Vinod Ashokan

Rodney Loudon (FRS)

Peter Töennies

Zygmunt Bak

Michel A. Ghantous

Elie Mojaes

Mehand Belhadi

Anastasia Parii

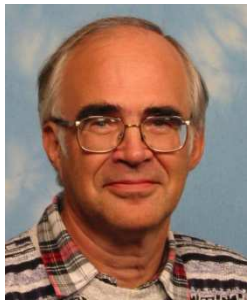

Klaus Maschke

Bernard Salanon

Jacob Szeftel

Scientific Collaborations